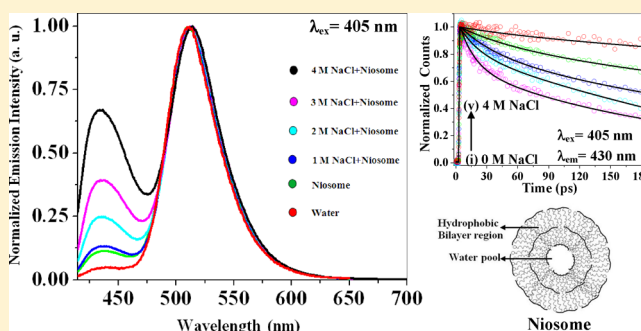


# Salt Effect on the Ultrafast Proton Transfer in Niosome

Tridib Mondal, Shirsendu Ghosh, Atanu Kumar Das, Amit Kumar Mandal, and Kankan Bhattacharyya\*

Department of Physical Chemistry, Indian Association for the Cultivation of Science, Jadavpur, Kolkata 700032, India

**ABSTRACT:** Excited state proton transfer (ESPT) of pyranine (8-hydroxypyranine-1,3,6-trisulfonate, HPTS) in a niosome is studied by fluorescence correlation spectroscopy (FCS) and femtosecond up-conversion. The niosome consists of a neutral surfactant triton X-100 (TX-100) and cholesterol. FCS studies suggest that in the presence of niosome almost all of the HPTS is transferred to the niosome and the amount of free HPTS present in bulk water is negligible. The time constant of initial proton transfer ( $\tau_{PT}$ ) in niosome (40 ps) is  $\sim 8$  times slower than that (5 ps) in bulk water, while the time constants of recombination ( $\tau_{rec}$ ) and dissociation ( $\tau_{diss}$ ) are  $\sim 4$  times and  $\sim 1.5$  times slower in niosome, respectively. On addition of NaCl, the rate of ESPT is markedly retarded both in free water and in niosome. In the niosome,  $\tau_{PT}$  slows down to 80 ps in 1 M NaCl and 225 ps in 4 M NaCl.



## 1. INTRODUCTION

Proton transfer in a confined medium (e.g., ion channels) plays a key role in many biological processes.<sup>1</sup> Proton transfer from an acid (ROH) is controlled by solvation of the ejected proton and the deprotonated species (RO<sup>-</sup>).<sup>2–4</sup> There has been a long-standing interest to understand how water and ions affect proton transfer. Huppert and co-workers<sup>3a</sup> examined the effect of electrolytes (NaCl and MgCl<sub>2</sub>) on the rate of proton transfer from pyranine (8-hydroxypyranine-1,3,6-trisulfonate, HPTS) to bulk water. They suggested that the rate of proton transfer to water depends on the number of free water molecules present in the vicinity of the HPTS molecule (anion). In the absence of any salt in bulk water, a proton is transferred to a water cluster containing  $\geq 10$  water molecules.<sup>3a</sup> But in the presence of salt ( $>0.5$  M MgCl<sub>2</sub>) a large fraction of the water molecules remain bound to the ions because of strong electrostatic/hydrogen-bond interaction. As a result, the amount of free water molecules decreases and this causes marked retardation of ESPT.<sup>3a</sup> Nibbering and co-workers studied ESPT from HPTS to acetate using mid-IR femtosecond pulses.<sup>5</sup> They showed that proton transfer between HPTS and a directly hydrogen bonded acetate ion is faster than that between HPTS and an acetate separated by one or more water molecules. Mondal et al. showed that inside the nanocavity of  $\gamma$ -cyclodextrin, the ESPT process is slowed down because of slower solvation and the presence of two bridging water molecules separating HPTS and acetate.<sup>6a</sup>

Recently, many groups reported on ultrafast ESPT in confined media.<sup>2,7–12</sup> Fayer and co-workers studied ultrafast ESPT of HPTS in AOT microemulsion<sup>2a</sup> and nafen membrane.<sup>2b</sup> In bulk water, the rise of the RO<sup>-</sup> emission exhibits an initial  $\sim 1$  ps component that arises from solvation dynamics (Stokes shift) and this is followed by proton transfer with two time constants (3 and 88 ps).<sup>2a</sup> Huppert and co-

worker<sup>7a</sup> studied ESPT in AOT microemulsion and considered a diffusion model introduced by Agmon.<sup>4a</sup> Mondal et al.<sup>6b</sup> studied ESPT of HPTS to water in a cyclodextrin cavity using femtosecond up-conversion. Huppert and co-workers<sup>3b</sup> carried out a molecular dynamics (MD) simulation on ESPT of HPTS in a cyclodextrin cavity. Very recently, Douhal and co-workers reported proton transfer in zeolite nanocages<sup>8a</sup> and silicon mesoporous materials.<sup>8b</sup> Iyer et al.<sup>9a</sup> showed that the proton transfer in nafen membrane is significantly slowed down with decrease in the water content of the nafen membrane.

Niosomes are nonionic surfactant vesicles that are osmotically active.<sup>13</sup> They are structurally similar to liposomes. However, the bilayer of niosomes is made up of nonionic surfactant rather than phospholipids (as in the case of liposomes). Cholesterol or polyethylene glycol (PEG) increases the rigidity of the membrane of a niosome. There is a water pool at the core of a niosome. Thus, there are two different regions inside a niosome: a hydrophobic bilayer region and a hydrophilic core (water pool) region. Because of this, a niosome can encapsulate both hydrophobic and hydrophilic drug molecules and hence, niosomes have wide applications in drug delivery.

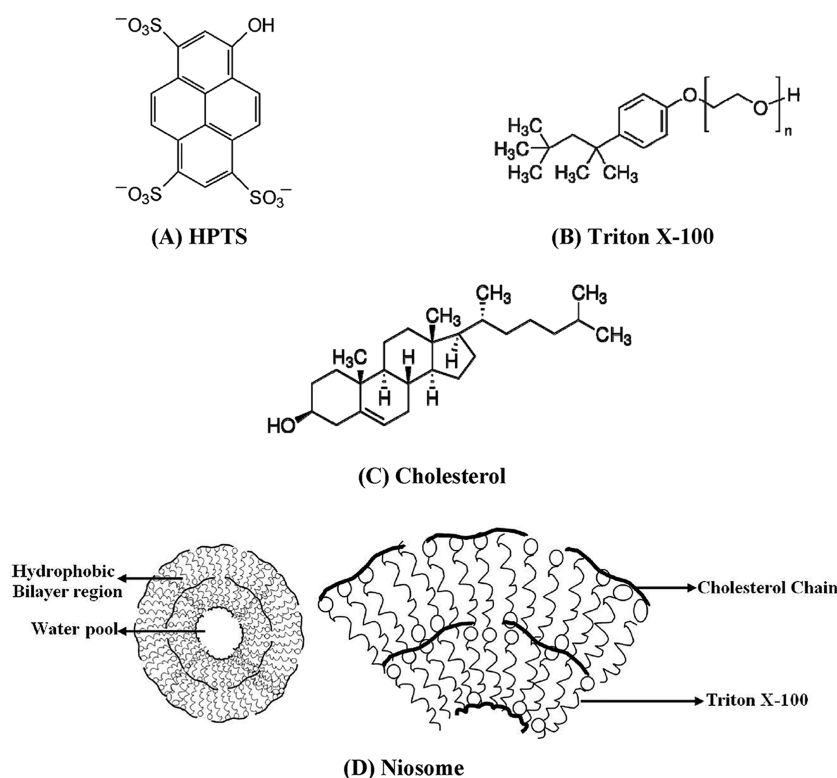
Bakker and co-workers<sup>14a</sup> studied the effect of salt on the ESPT process of HPTS to water and acetate by femtosecond transient electronic and vibrational spectroscopy. They found that addition of salt slows down proton transfer to H<sub>2</sub>O but does not affect the rate of proton transfer to acetate if HPTS is separated from acetate by more than two water molecules.<sup>14a</sup> Using fluorescence lifetime correlation spectroscopy, Paredes<sup>14b</sup> et al. demonstrated that in bulk water the anions affect

Received: May 7, 2012

Revised: June 25, 2012

Published: June 27, 2012

Scheme 1. Schematic Representation of (A) 8-Hydroxypyrene-1,3,6-trisulfonate (HPTS), (B) Triton X-100, (C) Cholesterol, and (D) Niosome<sup>17</sup>



ESPT more than the cations. They correlated the behavior of the different ions to the Hofmeister series.<sup>14b</sup> We have recently reported on ESPT in a room temperature ionic liquid (RTIL) mixed-micelle and microemulsion.<sup>10</sup> In this work, we report on the effect of NaCl on the ESPT process of HPTS (8-hydroxypyrene-1,3,6-trisulfonate) in a niosome. The ions affect the ESPT process in a number of ways. The strong electric field of the ions causes electrostriction and increases viscosity.<sup>15</sup> Neutron diffraction studies<sup>15a,b</sup> and simulations<sup>15c,d</sup> indicate that water structure is perturbed beyond the first solvation shell of the ions up to  $\sim 3$  layers.<sup>15</sup> This implies substantial disruption of the hydrogen bond network in water. The other effect of added salt is electrolytic screening.<sup>4</sup> This refers to the formation of an ionic atmosphere consisting of the added ions around the HPTS ion and its deprotonated form. This causes a screening of the coulomb attraction between  $\text{RO}^-$  and the ejected proton and affects the diffusion coefficient ( $D$ ) of the proton and the  $\text{RO}^-$ .<sup>3,4</sup> With increase in concentration ( $c$ ) of the electrolyte  $D$  decreases as  $1/\sqrt{C}$ .<sup>3,4</sup> Pradhan and Biswas<sup>16</sup> studied the effect of electrolyte on the rate of isomerization and intramolecular charge transfer (CT) reactions<sup>16a-c</sup> and on the size of reverse micelles.<sup>16d</sup> They applied Zwan–Hynes theory to explain the electrolyte concentration dependence.<sup>16a-c</sup> In the present work, we investigate the effect of salt on proton transfer inside a niosome.

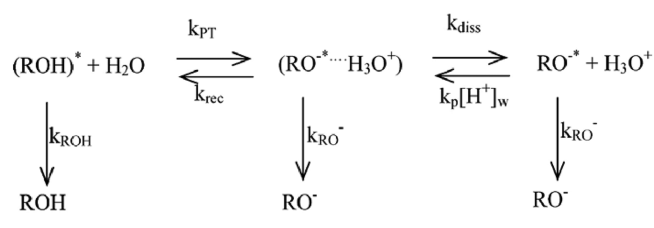
## 2. EXPERIMENTAL SECTION

Pyranine (8-hydroxypyrene-1,3,6-trisulfonate, HPTS, Scheme 1A) was purchased from Fluka and used without further purification. Triton X-100 (Scheme 1B), cholesterol (Scheme 1C) (Sigma Aldrich), and NaCl (Merck) were purchased and used as received.

The steady state absorption and emission spectra were recorded in a Shimadzu UV-2401 spectrophotometer and a Spex FluoroMax-3 spectrofluorimeter, respectively. Our femto-second up-conversion setup (FOG 100, CDP) and femto-second laser (Tsunami pumped by a 5 W Millennia, Spectra Physics) as well as the picosecond TCSPC setup have been described in detail in our previous publications.<sup>10</sup> All experiments were done at room temperature (293 K) and at  $\lambda_{\text{ex}} = 405 \text{ nm}$ .

In order to estimate the rate constants of proton transfer, we followed a simple kinetic scheme (Scheme 2) that was used

Scheme 2. Kinetic Scheme Depicting the Proton Transfer Process in Pyranine (HPTS)



earlier by several groups.<sup>2a,b,12</sup> According to this scheme, the excited state proton transfer (ESPT) process in a photoacid (ROH) involves three steps: initial proton transfer ( $k_{\text{PT}}$ ), recombination of the geminate ion pair ( $k_{\text{rec}}$ ), and dissociation of the geminate ion pair into a solvent-separated ion pair ( $k_{\text{diss}}$ ). The time evolution of the different species is described by the following coupled differential equations:<sup>2c</sup>

$$\frac{d}{dt} \begin{bmatrix} \text{ROH} \\ \text{RO}^- \cdots \text{H}^+ \\ \text{RO}^- \end{bmatrix} = \begin{bmatrix} -X & k_{\text{rec}} & 0 \\ k_{\text{PT}} & -Y & 0 \\ 0 & k_{\text{diss}} & -Z \end{bmatrix} \times \begin{bmatrix} \text{ROH} \\ \text{RO}^- \cdots \text{H}^+ \\ \text{RO}^- \end{bmatrix} \quad (1)$$

where

$$\begin{aligned} X &= k_{\text{PT}} + k_{\text{ROH}} \approx k_{\text{PT}} \\ Y &= k_{\text{rec}} + k_{\text{diss}} + k_{\text{RO}^-} \\ Z &= k_{\text{RO}^-} \end{aligned} \quad (2)$$

As discussed earlier, individual rate constants were calculated by using the amplitude and the time constants of the emission transient of ROH and  $\text{RO}^-$ .<sup>2a,b,12</sup> It may be mentioned that a recent FCS study<sup>17</sup> indicates that the microenvironment inside a niosome is quite homogeneous and hence, we used a single value of the rate constants.

The FCS studies of the samples were carried out in a confocal microscope (PicoQuant, Micro Time 200) with an inverted optical microscope (Olympus IX-71) and the methods of analysis are described in our previous publications.<sup>18</sup> The emission above 430 nm was collected by using a long pass filter (HQ430lp). The FCS experiment was done at room temperature (20 °C). To study FCS we have used ~1 nM HPTS in the niosome solution.

The autocorrelation function  $G(\tau)$  is defined as<sup>19</sup>

$$G(\tau) = \frac{\langle \delta F(0) \delta F(\tau) \rangle}{\langle F \rangle^2} \quad (3)$$

where  $\langle F \rangle$  is the average intensity and  $\delta F(\tau)$  is the fluctuation in the intensity at a delay  $\tau$  around the mean value, i.e.,  $\delta F(\tau) = \langle F \rangle - F(\tau)$ .

We fitted  $G(\tau)$  to a model with 3D diffusion having triplet contribution. In this model, the correlation function is expressed as<sup>19</sup>

$$G(\tau) = \frac{1 - T + T \exp(-\tau/\tau_{\text{tr}})}{N(1 - T)} (1 + \tau/\tau_{\text{D}})^{-1} (1 + \tau/\tau_{\text{D}} S^2)^{-1/2} \quad (4)$$

In this equation  $\tau_{\text{D}}$  denotes the diffusion time in the confocal volume,  $\tau_{\text{tr}}$  is the triplet lifetime of a dye molecule,  $T$  is the fraction of number of molecules in the triplet state,  $\tau$  is the delay time, and  $N$  represents the average number of molecules in the confocal volume.

The diffusion constant of the dyes can be determined by using the following equation

$$D_{\text{t}} = \frac{\omega_{\text{xy}}^2}{4\tau_{\text{D}}} \quad (5)$$

where,  $\omega_{\text{xy}}$  is the transverse radius (~305 nm) of the confocal volume (~0.8 fL). The number of HPTS molecules (anions) in the confocal volume was measured by using the  $G(0)$  value (~1/ $N$ ) of the autocorrelation function  $G(\tau)$  and we calculated that 12 molecules (anions) of HPTS are present inside the confocal volume.

**2.1. Preparation of Niosome.** Pozzi et al. reported formation of niosome by mixing Tween 20 and cholesterol.<sup>13a</sup> In this work, we followed their method to prepare niosomes using a different neutral surfactant (triton X-100, TX-100) and cholesterol. For this purpose, TX-100 and cholesterol were

taken in a molar ratio ~2:1, respectively. The samples were dissolved in a  $\text{CHCl}_3/\text{CH}_3\text{OH}$  (3:1 v/v) mixture in a round-bottomed flask. The concentration of TX-100 (~1.25 mM) was always above its critical micellar concentration ( $\text{CMC} \approx 0.22 \text{ mM}$ ).<sup>20</sup> The mixture was evaporated with use of a rotary evaporator for 2 h and then in a vacuum pump for about an hour at room temperature (20 °C). After the evaporation of the solvents, the dried film was hydrated by the addition of the required amount of distilled water. The dispersion was vortexed for 10 min and after that sonicated for 30 min.

### 3. RESULTS

**3.1. DLS Study.** Figure 1 shows size distribution of the niosome particles in the absence of salt and in the presence of 4

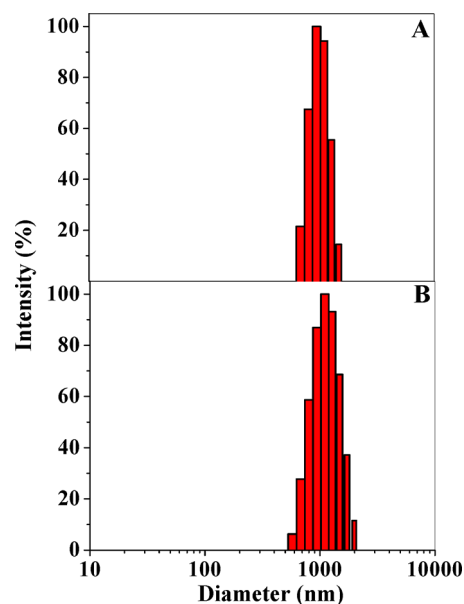


**Figure 1.** Size distribution of dynamic light scattering (DLS) study of niosome in the (A) absence and (B) presence of 4 M NaCl.

M NaCl obtained by using dynamic light scattering (DLS). The DLS data exhibit only one peak at ~1000 nm (Figure 1A). This suggests that this system (niosome) broadly consists of only one kind of particle of size ~1000 nm. On addition of NaCl, the diameter of the niosome remains almost the same (Figure 1B).

**3.2.1. FCS Study: Diffusion in Bulk Water.** In bulk water, the diffusion constant ( $D_{\text{t}}$ ) of HPTS is  $350 \mu\text{m}^2 \text{ s}^{-1}$  (Table 1, Figure 2A). On addition of 1 and 4 M NaCl the diffusion constant ( $D_{\text{t}}$ ) of HPTS in bulk water decreases to 310 and 215

**Table 1. Diffusion Constants of HPTS in Niosome and in Water in Different NaCl Concentration**

system	$D_{\text{t}} (\mu\text{m}^2 \text{ s}^{-1})$
niosome	40
niosome +1 M NaCl	30
niosome + 4 M NaCl <sup>a</sup>	16
water	350
water +1 M NaCl	310
water +4 M NaCl	215

<sup>a</sup>Contains 15% triplet contribution ( $T$ ). For other systems triplet contributions ( $T$ ) are <3%.

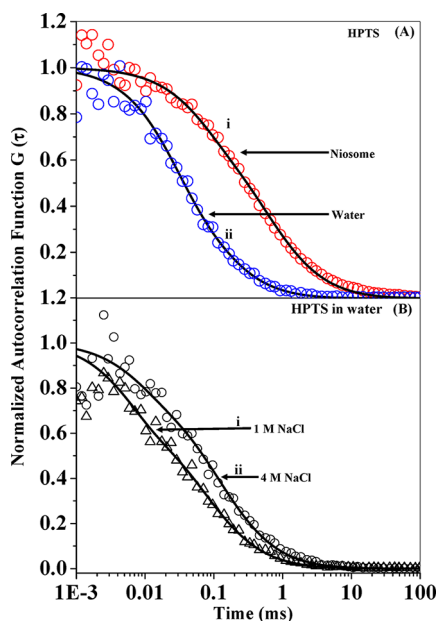


**Figure 2.** Comparison of autocorrelation traces of (A) (i) HPTS in niosome (surface immobilized) (red) and (ii) HPTS in water (blue) and (B) HPTS in water in the presence of (i) 1 M ( $\Delta$ ) and (ii) 4 M ( $\circ$ ) NaCl. Corresponding fitted lines are shown by the solid black lines.

$\mu\text{m}^2 \text{s}^{-1}$  respectively (Table 1, Figure 2B). Thus diffusion of HPTS in 4 M NaCl is  $\sim 1.5$  times slower than that in bulk water. The slower diffusion in 4 M NaCl may be attributed to 1.5 times increase in the viscosity of water on addition of 4 M NaCl.

**3.2.2. FCS Study: Diffusion Inside Niosome.** When an aqueous solution containing niosomes is placed on a glass surface, the niosomes sticks to the glass and become immobilized. No correlation was detected when the laser beam is focused in bulk solution and in this case (Figure 3A). This indicates that the number of free HPTS molecules (anions) outside niosome in the bulk solution is negligible and almost all the HPTS anions bind to the niosome.

Figure 2A shows the FCS (emission wavelength  $>430$  nm) curves of HPTS anion in a niosome immobilized on a glass surface.  $D_t$  of HPTS in niosome is  $\sim 8.5$  times smaller ( $\sim 40 \mu\text{m}^2 \text{s}^{-1}$ ) than in bulk water. Note, in this case the niosome is completely immobilized on the glass surface. Thus the lower value of  $D_t$  of HPTS inside niosome may be attributed to the higher friction inside niosome.

In the presence of 1 M NaCl the diffusion constant of HPTS in niosome becomes slightly smaller ( $30 \mu\text{m}^2 \text{s}^{-1}$ ) (Table 1, Figure 3B) than that in niosome alone ( $40 \mu\text{m}^2 \text{s}^{-1}$ ). However, in the presence of 4 M NaCl, the diffusion constant of HPTS in niosome becomes  $16 \mu\text{m}^2 \text{s}^{-1}$  (Table 1, Figure 3B), which is  $\sim 2.5$  times smaller than that in niosome. This indicates that the penetration of  $\text{Na}^+$  and  $\text{Cl}^-$  ions inside niosome increases local friction  $\sim 2.5$  times. Note, in the case of 4 M NaCl the initial part of decay of  $G(\tau)$  contains a contribution of the triplet state (Table 1).

**3.3. Steady State Spectra in Bulk.** The steady state emission spectrum is a good indicator of the efficiency of the ESPT process. In bulk water, HPTS exhibits an intense emission peak at 520 nm due to the deprotonated form ( $\text{RO}^-$ ) and a weak emission peak at 430 nm due to the protonated form (ROH) form.

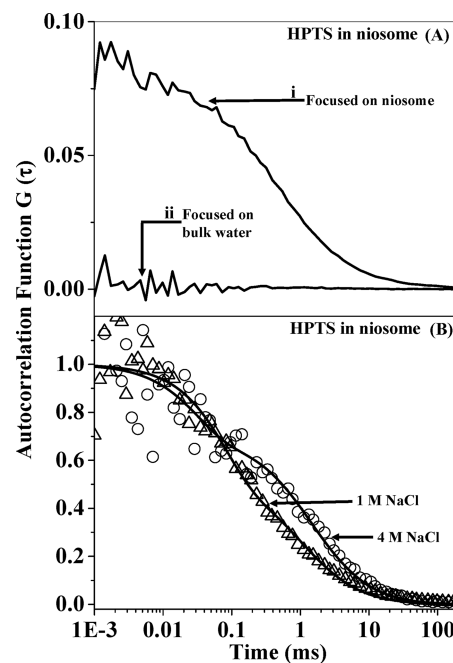


**Figure 3.** Comparison of autocorrelation traces of (A) (i) HPTS in niosome (surface immobilized) and (ii) HPTS in niosome (bulk focusing) and (B) HPTS in niosome in the presence of 1 M ( $\Delta$ ) and 4 M ( $\circ$ ) NaCl. Corresponding fitted lines are shown by the solid black lines.

Figure 4 shows the emission spectra in niosome and in the presence of NaCl at different concentrations (Table 2). In bulk

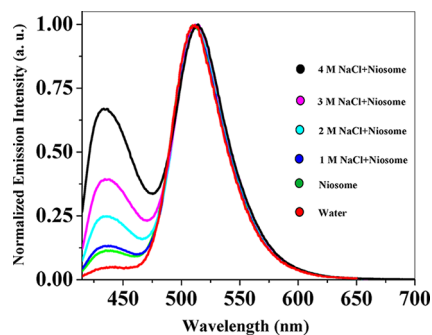


**Figure 4.** Steady state emission spectra of HPTS in water, niosome, and niosome in the presence of different NaCl concentrations (1–4 M) at  $\lambda_{\text{ex}} = 405$  nm.

water, because of ultrafast ESPT, the intensity of emission of the deprotonated form of HPTS ( $\text{RO}^-$ ,  $\lambda_{\text{em}} = 513$  nm) is about

**Table 2.** Ratio of Emission Intensity of  $\text{RO}^-$  Emission (at 530 nm) to ROH Emission (at 430 nm) of HPTS in Niosome in the Presence of NaCl

system	$I_{\text{RO}^-}/I_{\text{ROH}}$
water <sup>a</sup>	25
niosome	8.5
niosome + 1 M NaCl	7.5
niosome + 2 M NaCl	4.0
niosome + 3 M NaCl	2.5
niosome + 4 M NaCl	1.5

<sup>a</sup>See ref 10a.



25 times larger than that from the protonated form (ROH at  $\lambda_{\text{em}} = 430$  nm), i.e.  $I_{\text{RO}^-}/I_{\text{ROH}}$  is 25. In niosome, the  $I_{\text{RO}^-}/I_{\text{ROH}}$  ratio is nearly 3-fold reduced to 8.5 (Figure 4 and Table 2). The reduction in the  $I_{\text{RO}^-}/I_{\text{ROH}}$  ratio suggests that ESPT process inside the niosome is slower than that in water.

Addition of NaCl causes a further decrease in the  $I_{\text{RO}^-}/I_{\text{ROH}}$  ratio of HPTS in niosome. In the niosome, the ratio  $I_{\text{RO}^-}/I_{\text{ROH}}$  decreases from 8.5 in 0 M NaCl to 7.5 in 1 M NaCl and to 1.5 in 4 M NaCl. Figure 5 shows the variation of  $I_{\text{RO}^-}/I_{\text{ROH}}$  at

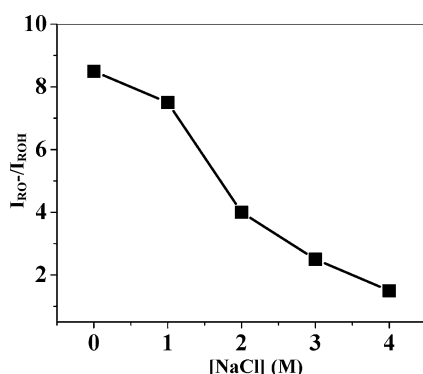


**Figure 5.** Plot of  $I_{\text{RO}^-}/I_{\text{ROH}}$  vs different concentrations of NaCl in the niosome.

different concentrations of NaCl in niosome. The marked effect of NaCl on ESPT in niosome suggests that a significant amount of NaCl is present inside the niosome and the presence of NaCl reduces the rate of ESPT.

**3.4. Picosecond and Femtosecond Study of Fluorescence from ROH and RO<sup>-</sup> in Bulk.** The steady state emission spectra give a qualitative picture of how NaCl affects the rate of ESPT in niosome. The rate constants of the primary steps of ESPT are obtained from picosecond and femtosecond studies. The fluorescence decays of the protonated form (ROH) were monitored at 430 nm, while those for the deprotonated form (RO<sup>-</sup>) are recorded at 530 nm. The ESPT process involves both ultrafast ( $\sim 1.5$  ps) and slow ( $\sim 400$  ps) time scales. The slow time constants are obtained in a picosecond TCSPC setup, and the ultrafast ones are obtained in a femtosecond up-conversion setup.

**3.4.1. Picosecond Time-Resolved Studies.** In bulk water, the emission at 530 nm (from the deprotonated form RO<sup>-</sup> of HPTS) exhibits a rise of time constant, 90 ps. In niosome, the longest time constant of rise of RO<sup>-</sup> increases to 190 ps. Thus the ESPT process is slowed down compared to that in bulk water.

On addition of NaCl to niosome, the deprotonated form of HPTS (RO<sup>-</sup>) exhibits a rise component, which is much longer than the 90 ps component in bulk water (Table 3). Figure 6 shows the fluorescence transients of HPTS at 430 nm (ROH emission) and at 530 nm (RO<sup>-</sup> emission) in the niosome both in the absence and presence of NaCl. In the presence of 4 M NaCl, the rise component increases to 675 ps, which is  $\sim 7.5$  times longer (slower) than that in bulk water and  $\sim 3.5$  times slower than that in niosome (Table 3, Figure 6B). Thus presence of NaCl markedly slows down the ESPT processes in niosome.

**3.4.2. Femtosecond Time-Resolved Studies.** In bulk water, femtosecond decay of ROH emission (at  $\lambda_{\text{em}} = 430$  nm) exhibits a 4-exponential decay with an ultrafast subpicosecond component (0.3 ps), two fast components (3 and 90 ps), and a

**Table 3. Picosecond Decay Parameters of the ROH Emission (at 430 nm) and the RO<sup>-</sup> Emission (at 530 nm) of HPTS in Different Systems**

system	$\lambda_{\text{em}}$ (nm)	$\tau_1^a$ (ps) ( $a_1$ )	$\tau_2^a$ (ps) ( $a_2$ )
niosome	430	190 (0.79)	2500 (0.21)
	530	190 (-0.62)	5770 (1.62)
niosome + 1 M NaCl	430	280 (0.78)	2550 (0.22)
	530	280 (-1.04)	5750 (2.04)
niosome + 2 M NaCl	430	390 (0.72)	2700 (0.28)
	530	390 (-1.03)	6000 (2.03)
niosome + 3 M NaCl	430	420 (0.51)	2900 (0.49)
	530	420 (-2.71)	6500 (3.71)
niosome + 4 M NaCl	430	675 (0.44)	3000 (0.56)
	530	675 (-1.19)	6250 (2.19)

<sup>a</sup>  $\pm 10\%$ .

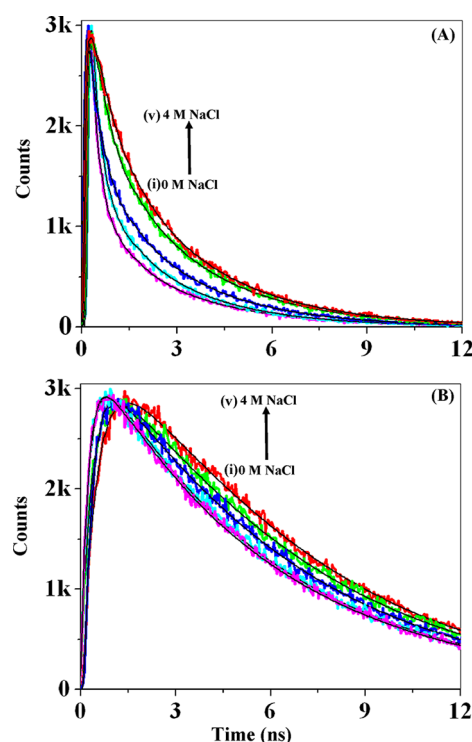


**Figure 6.** Picosecond transients of (A) ROH emission ( $\lambda_{\text{em}} = 430$  nm) and (B) anionic (RO<sup>-</sup>) emission ( $\lambda_{\text{em}} = 530$  nm) of HPTS in (i) niosome (magenta), niosome in the presence of (ii) 1 M NaCl (cyan), (iii) 2 M NaCl (blue), (iv) 3 M NaCl (green), and (v) 4 M NaCl (red), respectively, at  $\lambda_{\text{ex}} = 405$  nm. Corresponding fitted lines are shown by the solid black lines.

relatively slow (750 ps) component. Figure 7A shows the femtosecond transients of HPTS at 430 nm (ROH emission) in the niosome both in the absence and presence of NaCl. As shown in Figure 7A and Table 4, the decay components are 1, 15, 190, and 2500 ps in niosome in the absence of salt. On addition of 4 M NaCl, the decay components increase to 1.6, 62, 675, and 3000 ps, respectively.

In bulk water, the RO<sup>-</sup> emission at  $\lambda_{\text{em}} = 530$  nm displays three rise components of 0.3, 3, and 90 ps that match with the decay components of ROH. In niosome, the long rise time component increases to 190 ps, which is  $\sim 2$  times longer than that (90 ps) in water (Figure 7B). In addition to this long rise, we observed two other ultrafast rise times: 1 and 15 ps in the niosome in the absence of NaCl (Table 4).

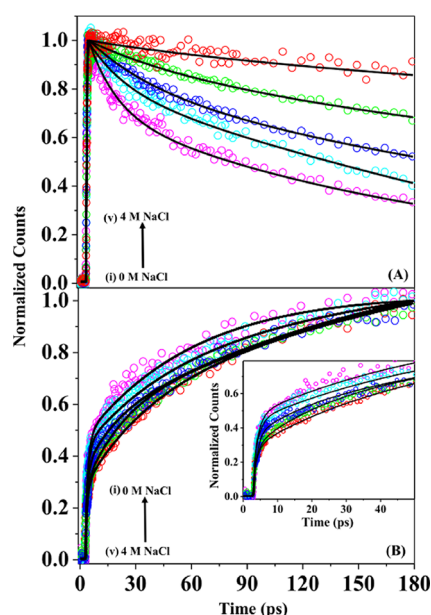


**Figure 7.** Femtosecond transients of (A) ROH emission ( $\lambda_{\text{em}} = 430$  nm) and (B)  $\text{RO}^-$  emission ( $\lambda_{\text{em}} = 530$  nm) of HPTS in (i) niosome (magenta), niosome in the presence of (ii) 1 M NaCl (cyan), (iii) 2 M NaCl (blue), (iv) 3 M NaCl (green), and (v) 4 M NaCl (red), respectively, at  $\lambda_{\text{ex}} = 405$  nm. Corresponding fitted lines are shown by the solid black lines. The inset of B shows the expanded view of the  $\text{RO}^-$  emission transients.

In the niosome, the long component of rise at 530 nm increases to 280 ps 1 M NaCl (i.e.,  $\sim 1.5$  times longer than that in 0 M NaCl). The faster components of rise increase to 1.2 and 22 ps in 1 M NaCl (Table 4, Figure 7B). In the presence of 4 M NaCl, the long rise increases up to 675 ps and the other rise components increase to 1.6 and 62 ps (Table 4). It may be noted the rise times at 530 nm correlate well with the decay constants observed at 430 nm.

#### 4. DISCUSSION

The most important finding of this work is the dramatic dependence of rates of ESPT in niosome on addition of NaCl. The time constants  $\tau_{\text{PT}} (=1/k_{\text{PT}})$ ,  $\tau_{\text{rec}} (=1/k_{\text{rec}})$ , and  $\tau_{\text{diss}} (=1/k_{\text{diss}})$  (calculated by using scheme 2 and eq 2) at different NaCl concentrations are summarized in Table 5.

Before we compare the time constants of the different steps in ESPT we will briefly discuss the factors that control these

**Table 5.** Time Constants of Deprotonation ( $\tau_{\text{PT}}$ ) of the Protonated Species (ROH), Recombination ( $\tau_{\text{rec}}$ ), and Dissociation ( $\tau_{\text{diss}}$ ) of Geminate Ion Pair of HPTS in Niosome at Different NaCl Concentrations

system	$\tau_{\text{PT}}$ (ps)	$\tau_{\text{rec}}$ (ps)	$\tau_{\text{diss}}$ (ps)
bulk water <sup>a</sup>	5	7	50
niosome	40	30	75
niosome + 1 M NaCl	80	40	80
niosome + 2 M NaCl	130	70	110
niosome + 3 M NaCl	185	110	115
niosome + 4 M NaCl	225	130	195

<sup>a</sup>See ref 10a.

processes. This first step, namely initial proton transfer ( $\tau_{\text{PT}}$ ), depends on solvation of the ejected proton and the deprotonated form ( $\text{RO}^-$ ). This depends on the dielectric constant, solvation dynamics, and availability of an adequate number of water molecules.

The dielectric constant is determined by the ability of the water molecules to reorient under an electric field. The confinement causes a decrease in dielectric constant in two ways. The first is the finite size of the cavity<sup>21a</sup> and the second is the disruption of the water–water hydrogen bond and consequent hampering of dynamic polarization.<sup>21b</sup> The reduction in dielectric constant inside niosome is confirmed by the blue shift of the emission maximum of coumarin dye (C153) in niosome (526 nm)<sup>22a</sup> compared to bulk water (547 nm).

Addition of small ions with a high electric field decreases the ability of a water molecule to reorient and, hence, causes further reduction in the dielectric constant. As a result, the solvation energy of a proton and  $\text{RO}^-$  in the presence of salt is lower than that in the absence of salt. This disfavors proton transfer in the presence of salt.

The second factor is solvation dynamics. Solvation dynamics in a niosome ( $\langle\tau_{\text{sol}}\rangle \approx 1675$  ps) is more than  $\sim 1000$ -fold slower<sup>22a</sup> compared to that of bulk water (1 ps).<sup>22b</sup> The slower rate of initial proton transfer in niosome may be due to slower solvation in niosome compared to bulk water. It may be recalled that Huppert et al.<sup>23a,b</sup> earlier reported that solvation by ions is very slow and applied Debye–Falkenhagen theory to explain ionic solvation.<sup>23,24</sup>

According to Huppert et al.<sup>3a</sup> in bulk water a proton needs at least  $>10$  water molecules to stabilize. The deprotonated form  $\text{RO}^-$  also needs a lot of water molecules to stabilize by

**Table 4.** Femtosecond Decay Parameters of the ROH Emission (at 430 nm) and the  $\text{RO}^-$  Emission (at 530 nm) of HPTS in Different Systems

system	$\lambda_{\text{em}}$ (nm)	$\tau_1^a$ (ps) ( $a_1$ )	$\tau_2^a$ (ps) ( $a_2$ )	$\tau_3^a$ (ps) ( $a_3$ )	$\tau_4^a$ (ps) ( $a_4$ )
niosome	430	1 (0.01)	15 (0.3)	190 (0.61)	2500 (0.08)
	530	1 (−0.22)	15 (−0.13)	190 (−0.65)	5770 (1.94)
niosome + 1 M NaCl	430	1.20 (0.008)	22 (0.2)	280 (0.75)	2550 (0.042)
	530	1.20 (−0.2)	22 (−1.61)	280 (−3.865)	5750 (6.675)
niosome + 2 M NaCl	430	1.35 (0.004)	35 (0.19)	390 (0.78)	2700 (0.026)
	530	1.35 (−0.2)	35 (−1.92)	390 (−4.33)	6000 (7.45)
niosome + 3 M NaCl	430	1.50 (0.004)	48 (0.11)	420 (0.56)	2900 (0.326)
	530	1.50 (−1.80)	48 (−2.32)	420 (−4.63)	6500 (9.75)
niosome + 4 M NaCl	430	1.60 (0.001)	62 (0.04)	675 (0.155)	3000 (0.804)
	530	1.60 (−0.92)	62 (−2.34)	675 (−0.067)	6250 (4.327)

<sup>a</sup> $\pm 10\%$ .

solvation. In the case of ESPT in 1-naphthol, Fuji and co-workers showed that at least 30 water molecules are needed to solvate the ejected proton and  $\text{RO}^-$ .<sup>25</sup> The  $\text{RO}^-$  form of HPTS contains  $-4$  charge and hence, may need more water molecules than 1-naphtholate anion (with  $-1$  charge). In summary,  $>30$  water molecules are needed for proton transfer of HPTS. So many water molecules may not be available in a niosome for the following reasons. The main constituents of the niosome are cholesterol and the surfactant (TX-100). Of these, cholesterol is highly hydrophobic with hydrocarbon rings and only one OH group (Scheme 1C). The surfactant contains a hydrophobic aromatic ring, only one OH, and several ether oxygen atoms (Scheme 1B). As a result, the number of water molecules inside the niosome is fewer than that around HPTS in bulk water.

The presence of ions causes a further decrease in the amount of free water. The strong electrostatic attraction of water molecules by  $\text{Na}^+$  and  $\text{Cl}^-$ , and the resulting hydration of the ions, decrease the number of relatively free water molecules available for stabilization of the ejected proton and  $\text{RO}^-$ . The number of water molecules around HPTS in niosome is already low for reasons discussed above (shielding by TX-100 and cholesterol). The presence of ions inside a niosome reduces the number of available water molecules further.

We now compare the time constant of initial proton transfer ( $\tau_{\text{PT}}$ ) in different systems. The time constant of initial proton transfer ( $\tau_{\text{PT}}$ ) is 5 ps in bulk water<sup>10a</sup> and 40 ps in niosome (8-fold slower). The slower rate of initial proton transfer may be ascribed to the lower dielectric constant, slower solvation, and reduction in the number of water molecules available for solvation of ejected proton and  $\text{RO}^-$ .

Let us now discuss the effect of NaCl in bulk water and niosome. In niosome, the time constant of initial proton transfer  $\tau_{\text{PT}}$  increases linearly (Figure 8A) with the concentration of the NaCl, from 40 ps at 0 M NaCl to 80 ps ( $\sim 2$ -fold) at 1 M NaCl and to 225 ps ( $\sim 6$ -fold) at 4 M NaCl. The magnitude of retardation in proton transfer (increase in time constant) is larger than that observed in bulk water by Huppert and co-workers ( $\sim 2.4$  times from 0 to 4 M NaCl).<sup>3a</sup> This may be explained in terms of the factors (dielectric constant, solvation dynamics, and number of free water molecules) discussed above.

The lower dielectric constant inside the niosome is expected to increase Coulomb attraction between  $\text{RO}^-$  and the ejected proton and may accelerate the rate of recombination. The observed slower rate of recombination is contrary to this and may be explained as follows. The recombination process involves a slight movement of the hydrogen-bonded ejected proton by less than one angstrom. In the case of water, the  $\text{RO}^-$  is hydrogen bonded to more than one hydrogen atom (apart from the ejected proton) and as a result the probability of recombination is high. Inside the niosome (Scheme 1D), the cholesterol (Scheme 1C) and the surfactant chains (TX-100) (Scheme 1B) shield HPTS from bulk water. Thus for most HPTS, the proton is transferred to the OH group of cholesterol and ethereal oxygen atoms of TX-100 chains.<sup>10b</sup> In such a case, there is only one proton (the ejected proton) available for recombination. This makes recombination slower in niosome compared to bulk water. Thus, in niosome, the time constant of recombination ( $\tau_{\text{rec}}$ ) is  $\sim 4$  times slower (30 ps) than that in bulk water (7 ps).

On addition of 1 M NaCl to niosome,  $\tau_{\text{rec}}$  becomes slightly slower (40 ps) compared to that (30 ps) in niosome. In the

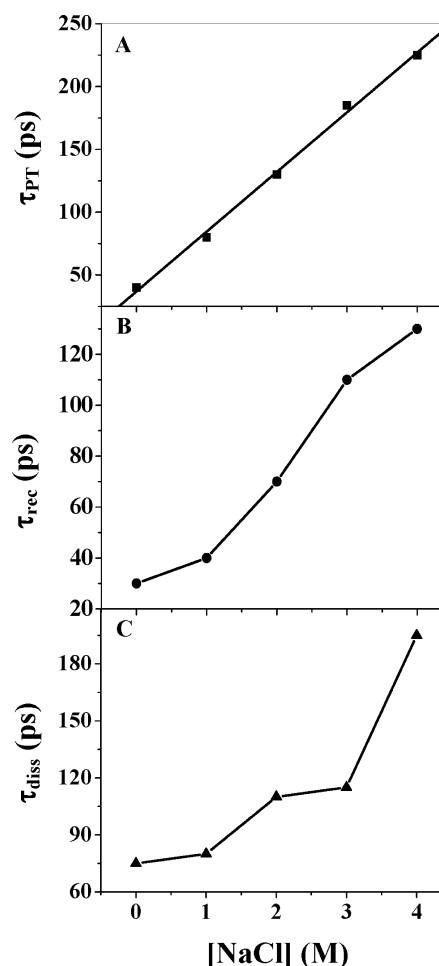


**Figure 8.** Plots of (A) time constant for initial proton transfer ( $\tau_{\text{PT}}$ ), (B) time constant for recombination ( $\tau_{\text{rec}}$ ), and (C) time constant for dissociation ( $\tau_{\text{diss}}$ ) vs different concentrations of NaCl.

presence of 4 M NaCl, the recombination time increases nearly 4-fold to 130 ps (Figure 8B). This is in sharp contrast to the nearly 2-fold decrease in time constant (i.e., acceleration) of recombination in bulk water. Inside the small volume of a niosome, the presence of the ionic atmosphere of NaCl and the strong attraction of the large number of  $\text{Na}^+$  ions shield HPTS anion from the ejected proton and this may retard the recombination.

The time constant of dissociation of the ion pair ( $\tau_{\text{diss}}$ ) depends on diffusion of the ejected proton (hydronium ion) and  $\text{RO}^-$ . In this case, the slower diffusion of  $\text{RO}^-$  may be rate determining. As suggested by the FCS data, diffusion of HPTS in niosome is  $\sim 8.5$  times slower than bulk water and is further retarded on addition of NaCl (section 3.2.2). As a result of this,  $\tau_{\text{diss}}$  in niosome (75 ps) is slightly slower than that in bulk water (50 ps). Addition of NaCl to niosome causes an increase the time constant of dissociation from 75 ps in 0 M NaCl, to 80 ps in 1 M NaCl and to 195 ps in 4 M NaCl (Figure 8C).

## 5. CONCLUSION

This work shows that the time constant for proton transfer, recombination, and dissociation in a niosome is  $\sim 2$ – $8$  fold slower compared to bulk water. This is attributed to slower solvation, shielding of HPTS by TX-100 and cholesterol from water, slower diffusion of  $\text{RO}^-$ , lower dielectric constant, and higher friction inside a niosome compared to bulk water. On



addition of NaCl the local friction increases further and the time scales ( $\tau_{PT}$ ,  $\tau_{re}$  and  $\tau_{diss}$ ) become slower. This is attributed to a decrease in the number of water molecules available for solvation of proton and deprotonated species and also to ionic solvation and increase of friction (slower diffusion) caused by NaCl.

## AUTHOR INFORMATION

### Corresponding Author

\*E-mail: pckb@iacs.res.in. Fax: (91)-33-2473-2805.

### Notes

The authors declare no competing financial interest.

## ACKNOWLEDGMENTS

Thanks are due to Department of Science and Technology, India (Centre for Ultrafast Spectroscopy and Microscopy and J. C. Bose Fellowship) and Council of Scientific and Industrial Research (CSIR) for generous research support. T.M., S.G., A.K.D., and A.K.M. thank CSIR for awarding fellowships.

## REFERENCES

- (1) (a) MacKinnon, R. Nobel Lecture, December 8, 2003: Morais-Cabral, J. H.; Zhou, Y.; MacKinnon, R. *Nature* **2001**, *414*, 37–42. (b) Wyatt, D. L.; de Godoy, C. M. G.; Cukierman, S. J. *Phys. Chem. B* **2009**, *113*, 6725–6731. (c) Rappaport, F.; Boussac, A.; Force, D. A.; Peloquin, J.; Brynda, M.; Sugiura, M.; Un, S.; Britt, R. D.; Diner, B. A. *J. Am. Chem. Soc.* **2009**, *131*, 4425–4433. (d) Riccardi, D.; König, P.; Prat-Resina, X.; Yu, H.; Elstner, M.; Frauenheim, T.; Cui, Q. *J. Am. Chem. Soc.* **2006**, *128*, 16302–16311. (e) Faxe, K.; Gilderson, G.; Adelroth, P.; Brzezinski, P. *Nature* **2005**, *437*, 286–289. (f) Cymes, G. D.; Ni, Y.; Grosman, C. *Nature* **2005**, *438*, 975–980. (g) Kuhlbrandt, W. *Nature* **2000**, *406*, 569–570. (h) Zscherp, C.; Schlesinger, R.; Tittor, J.; Oesterhelt, D.; Heberle, J. *Proc. Natl. Acad. Sci. U.S.A.* **1999**, *96*, 5498–5503. (i) Kotlyar, A. B.; Borovok, N.; Kiryati, S.; Nachliel, E.; Gutman, M. *Biochemistry* **1994**, *33*, 873–879.
- (2) (a) Spry, D. B.; Goun, A.; Fayer, M. D. *J. Phys. Chem. A* **2007**, *111*, 230–237. (b) Spry, D. B.; Goun, A.; Glusac, K.; Moilanen, D. E.; Fayer, M. D. *J. Am. Chem. Soc.* **2007**, *129*, 8122–8130. (c) Giestas, L.; Yihwa, C.; Lima, J. C.; Vautier-Giongo, C.; Lopes, A.; Macanita, A. L.; Quina, F. H. *J. Phys. Chem. A* **2003**, *107*, 3263–3269.
- (3) (a) Leiderman, P.; Gepshtein, R.; Uritski, A.; Genosar, L.; Huppert, D. *J. Phys. Chem. A* **2006**, *110*, 5573–5584. (b) Gepshtein, R.; Leiderman, P.; Huppert, D.; Project, E.; Nachliel, E.; Gutman, M. *J. Phys. Chem. B* **2006**, *110*, 26354–26364.
- (4) (a) Agmon, N. *J. Phys. Chem. A* **2005**, *109*, 13–35. (b) Uritski, A.; Leiderman, P.; Huppert, D. *J. Phys. Chem. A* **2006**, *110*, 13686–13695. (c) Maurer, P.; Thomas, V.; Rivard, U.; Ifitime, R. *J. Chem. Phys.* **2010**, *133*, 044108 (1–8).
- (5) (a) Rini, M.; Magnes, B.-Z.; Pines, E.; Nibbering, E. T. J. *Science* **2003**, *301*, 349–352. (b) Mohammed, O. F.; Pines, D.; Dreyer, J.; Pines, E.; Nibbering, E. T. J. *Science* **2005**, *310*, 83–86. (c) Mohammed, O. F.; Dreyer, J.; Magnes, B.-Z.; Pines, E.; Nibbering, E. T. J. *ChemPhysChem* **2005**, *6*, 625–636.
- (6) (a) Mondal, S. K.; Sahu, K.; Ghosh, S.; Sen, P.; Bhattacharyya, K. *J. Phys. Chem. A* **2006**, *110*, 13646–13652. (b) Mondal, S. K.; Sahu, K.; Sen, P.; Roy, D.; Ghosh, S.; Bhattacharyya, K. *Chem. Phys. Lett.* **2005**, *412*, 228–234.
- (7) (a) Cohen, B.; Huppert, D.; Solntsev, K. M.; Tsfadia, Y.; Nachliel, E.; Gutman, M. *J. Am. Chem. Soc.* **2002**, *124*, 7539–7547. (b) Pines, E.; Huppert, D.; Agmon, N. *J. Chem. Phys.* **1988**, *88*, 5620–5630.
- (8) (a) Gil, M.; Ziölek, M.; Organero, J. A.; Douhal, A. *J. Phys. Chem. C* **2010**, *114*, 9554–9562. (b) Cohen, B.; Wang, S.; Organero, J. A.; Campo, L. F.; Sanchez, F.; Douhal, A. *J. Phys. Chem. C* **2010**, *114*, 6281–6289. (c) Douhal, A.; Angulo, G.; Gil, M.; Organero, J. A.; Sanz, M.; Tormo, L. *J. Phys. Chem. B* **2007**, *111*, 5487–5493. (d) Douhal, A. *Acc. Chem. Res.* **2004**, *37*, 349–355. (e) Douhal, A. *Chem. Rev.* **2004**, *104*, 1955–1976. (f) Cohen, B.; Alvarez, C. M.; Carmona, N. A.; Organero, J. A.; Douhal, A. *J. Phys. Chem. B* **2011**, *115*, 7637–7647.
- (9) (a) Iyer, E. S. S.; Datta, A. *J. Phys. Chem. B* **2011**, *115*, 8707–8712. (b) Iyer, E. S. S.; Datta, A. *J. Phys. Chem. B* **2012**, *116*, 5302–5307.
- (10) (a) Mondal, T.; Das, A. K.; Sasmal, D. K.; Bhattacharyya, K. *J. Phys. Chem. B* **2010**, *114*, 13136–13142. (b) Sen Mojumdar, S.; Mondal, T.; Das, A. K.; Dey, S.; Bhattacharyya, K. *J. Chem. Phys.* **2010**, *132*, 194505 (1–8).
- (11) Genosar, L.; Cohen, B.; Huppert, D. *J. Phys. Chem. A* **2000**, *104*, 6689–6698.
- (12) (a) Ghosh, S.; Dey, S.; Mandal, U.; Adhikari, A.; Mondal, S. K.; Bhattacharyya, K. *J. Phys. Chem. B* **2007**, *111*, 13504–13510. (b) Mondal, S. K.; Sahu, K.; Ghosh, S.; Sen, P.; Bhattacharyya, K. *J. Phys. Chem. A* **2006**, *110*, 13646–13652. (c) Roy, D.; Karmakar, R.; Mondal, S. K.; Sahu, K.; Bhattacharyya, K. *Chem. Phys. Lett.* **2004**, *399*, 147–151.
- (13) (a) Pozzi, D.; Caminiti, R.; Marianecci, C.; Carafa, M.; Santucci, E.; De Sanctis, S. C.; Caracciolo, G. *Langmuir* **2010**, *26*, 2268–2273. (b) Kato, K.; Walde, P.; Koine, N.; Ichikawa, S.; Ishikawa, T.; Nagahama, R.; Ishihara, T.; Tsujii, T.; Shudou, M.; Omokawa, Y.; Kuroiwa, T. *Langmuir* **2008**, *24*, 10762–10770. (c) Manconi, M.; Sinico, C.; Valenti, D.; Lai, F.; Fadda, A. M. *Int. J. Pharm.* **2006**, *311*, 11–19. (d) Sennato, S.; Bordini, F.; Cametti, C.; Marianecci, C.; Carafa, M.; Cametti, M. *J. Phys. Chem. B* **2008**, *112*, 3720–3727. (e) Lo, C. T.; Jahn, A.; Locascio, L. E.; Vreeland, W. N. *Langmuir* **2010**, *26*, 8559–8566.
- (14) (a) Cox, M. J.; Siwick, B. J.; Bakker, H. J. *ChemPhysChem* **2009**, *10*, 236–244. (b) Paredes, J. M.; Garzon, A.; Crovetto, L.; Orte, A.; Lopez, S. G.; Alvarez-Pez, J. M. *J. Phys. Chem. Chem. Phys.* **2012**, *14*, 5795–5800.
- (15) (a) Mancinelli, R.; Botti, A.; Bruni, F.; Ricci, M. A.; Soper, A. K. *J. Phys. Chem. B* **2007**, *111*, 13570–13577. (b) Mancinelli, R.; Botti, A.; Bruni, F.; Riccia, M. A.; Soper, A. K. *J. Phys. Chem. Chem. Phys.* **2007**, *9*, 2959–2967. (c) Chandra, A. *Phys. Rev. Lett.* **2000**, *85*, 768–771. (d) Carrillo-Tripp, M.; Saint-Martin, H.; Ortega-Blake, I. *J. Chem. Phys.* **2003**, *118*, 7062–7073.
- (16) (a) Pradhan, T.; Gazi, H. A. R.; Biswas, R. *J. Chem. Phys.* **2009**, *131*, 054507. (1–9). (b) Pradhan, T.; Biswas, R. *J. Phys. Chem. A* **2007**, *111*, 11514–11523. (c) Pradhan, T.; Biswas, R. *J. Phys. Chem. A* **2007**, *111*, 11524–11530. (d) Pradhan, T.; Gazi, H. A. R.; Guchhait, B.; Biswas, R. *J. Chem. Sci.* **2012**, *124*, 355–373.
- (17) Ghosh, S.; Mandal, A. K.; Das, A. K.; Mondal, T.; Bhattacharyya, K. *J. Phys. Chem. Chem. Phys.* **2012**, *14*, 9749–9757.
- (18) Sasmal, D. K.; Mandal, A. K.; Mondal, T.; Bhattacharyya, K. *J. Phys. Chem. B* **2011**, *115*, 7781–7787.
- (19) Lakowicz, J. R. *Principles of Fluorescence Spectroscopy*, 3rd ed; Springer: New York, 2006; Chapter 24.
- (20) Tiller, G. E.; Mueller, T. J.; Dockter, M. E.; Struve, W. G. *Anal. Biochem.* **1984**, *141*, 262–266.
- (21) (a) Senapati, S.; Chandra, A. *J. Phys. Chem. B* **2001**, *105*, 5106–5109. (b) Rick, S. W.; Stuart, S. J.; Berne, B. J. *J. Chem. Phys.* **1994**, *101*, 6141–6156.
- (22) (a) Ghatak, C.; Rao, V. G.; Ghosh, S.; Mandal, S.; Sarkar, N. *J. Phys. Chem. B* **2011**, *115*, 12514–12520. (b) Jimenez, R.; Fleming, G. R.; Kumar, P. V.; Maroncelli, M. *Nature* **1994**, *369*, 471–473.
- (23) (a) Bart, E.; Meltsin, A.; Huppert, D. *J. Phys. Chem.* **1994**, *98*, 10819–10823. (b) Argaman, R.; Molotsky, T.; Huppert, D. *J. Phys. Chem. A* **2000**, *104*, 7934–7943. (c) Kashyap, H. K.; Biswas, R. *J. Phys. Chem. B* **2010**, *114*, 16811–16823. (d) Ingram, J. A.; Moog, R. S.; Ito, N.; Biswas, R.; Maroncelli, M. *J. Phys. Chem. B* **2003**, *107*, 5926–5932.
- (24) (a) Bagchi, B.; Biswas, R. *Acc. Chem. Res.* **1998**, *31*, 181–187. (b) Biswas, R.; Roy, S.; Bagchi, B. *Phys. Rev. Lett.* **1995**, *75*, 1098–1101. (c) Biswas, R.; Bagchi, B. *J. Am. Chem. Soc.* **1997**, *119*, 5946–5952.
- (25) Saeki, M.; Ishiuchi, S.-I.; Sakai, M.; Fuji, M. *J. Phys. Chem. A* **2001**, *105*, 10045–10053.